Article ID: 1000-324X(2016)07-0779-06 **DOI:** 10.15541/jim20160030

Effects of HfO_2 Interlayer on Microstructure and Mechanical Property of Al_2O_3 Thin Film on MgF_2 Substrate

SONG Bo[1, 2], ZHAO Li-Li[1], CHEN Xiao-Ying[1], YOU Li-Jun[1], SONG Li-Xin[1]

(1. Key Laboratory of Inorganic Coating Materials, Shanghai Institute of Ceramics, Chinese Academy of Sciences, Shanghai 200050, China; 2. University of Chinese Academy of Sciences, Beijing 100049, China)

Abstract: Al_2O_3 thin films with or without HfO_2 interlayer between Al_2O_3 and substrate were deposited on MgF_2 substrates by electron-beam evaporation technique. The as-deposited thin films were then annealed at 600℃ for 1 h to promote crystallization. The microstructure, IR transmittance and mechanical properties of the as-deposited and annealed samples were investigated by field emission scanning electron microscopy (FE-SEM), grazing incidence X-ray diffraction (GIXRD), Fourier Transform Infrared (FTIR) spectrometer, nanoindentation, and scratch tests, respectively. FE-SEM results show that a new branch-like layer is generated in annealed HfO_2/Al_2O_3 double-layer thin films. The hardness of the newly formed layer is considered to be larger than 17.5 GPa. Because of the high hardness of the new layer, the MgF_2 substrate can be protected from being drown out during scratch test. From GIXRD patterns, Al_2O_3 still remains amorphous while HfO_2 interlayer transforms from amorphous to monoclinic phase after annealing process. It could be deduced that it is the phase transformation of HfO_2 interlayer that promotes the formation of the harder branch-like layer.

Key words: HfO_2 interlayer; Al_2O_3 thin film; microstructure; mechanical properties; MgF_2 substrate

MgF_2 is a widely used material for IR window applications due to its high transmittance in the range from 3 μm to 5 μm[1-2]. However, its low hardness and mechanical strength severely limit its application in harsh environments, as high speed vehicles may suffer from serious sand and rain erosions[3]. A commonly adopted way for improving the mechanical properties of IR windows is to coat a protective thin film on it. In the past decades, several materials such as diamond-like carbon (DLC)[4], oxides[5], phosphides[6], and nitrides[7] were often chosen due to their high mid-infrared transmittance and excellent environmental durability. Among these materials, one of the best choices for MgF_2 substrate is Al_2O_3, for the refractive index of Al_2O_3 is relatively small and subsequently the mid-IR transmittance loss can be minimized when deposited onto MgF_2.

Crystalline Al_2O_3 thin films are much harder and more wear-resistant than their amorphous counterpart. In particular, the thermodynamically stable α-Al_2O_3 has the most excellent mechanical properties and possesses the highest hardness up to 23 GPa[8]. However, it is very difficult to deposit hard crystalline Al_2O_3 thin films, especially the α-Al_2O_3 thin film. In the past, a lot of attempts in many ways including physical vapor deposition (PVD) and chemical vapor deposition (CVD) techniques have been dedicated to obtain crystalline Al_2O_3 thin films. A commercial way to deposit α-Al_2O_3 thin film is using CVD technique which requires a substrate temperature (T_s) of above 1000℃[9]. This high temperature may inevitably lead to degradation of the substrate with low melting point like glass, MgF_2. At T_s of 600–1000℃, the metastable crystalline γ, δ, θ and κ phases could be attained in the magnetron sputtering processes. Compared with magnetron sputtering, a much higher deposition rate could be achieved with electron-beam evaporation technique[10-11]. However, only amorphous Al_2O_3 thin films could be obtained by this process. Thus post crystallizing at elevated temperature was required for the thin film to improve mechanical properties[12]. It was found that amorphous Al_2O_3 converted into different metastable crystalline phases during annealing between 800℃ to 1100℃ and only annealing above 1100℃ resulted in α-Al_2O_3[13-14]. Other approaches which use template layers for the deposition of crystalline Al_2O_3 thin films have also been proposed[15-16]. α-Cr_2O_3 interlayer was found to promote the formation of α-Al_2O_3 at lower temperature. Apart from being able to

Received date: 2016-01-15; **Modified date:** 2016-03-25
Biography: SONG Bo(1989–), male, candidate of master degree. E-mail: songbo@shanghaitech.edu.cn
Corresponding author: SONG Li-Xin, professor. E-mail: lxsong@mail.sic.ac.cn

promote crystallization, annealing process can also increase the adhesion of thin film to substrate[17]. As for this work, the high temperatures mentioned above could cause pulverization of MgF_2 substrate. Thus a new way that combines annealing at relatively low temperature with HfO_2 interlayer is proposed.

In this work, Al_2O_3 thin films with or without HfO_2 interlayer between Al_2O_3 and substrate were prepared by electron-beam evaporation technique on MgF_2 substrates for protective purpose. The effects of HfO_2 interlayer on the microstructure and mechanical properties of Al_2O_3 thin film after annealing treatment were revealed. Moreover, the changes of optical and mechanical properties were discussed in relation with the microstructures.

1 Experimental

Al_2O_3 thin films with or without HfO_2 interlayer between Al_2O_3 and substrate were deposited on MgF_2 substrates by electron-beam evaporation technique with the thickness of 1260 nm (50 nm for HfO_2 interlayer). The MgF_2 substrates were cleaned by three steps including alcohol, acetone and distilled water in ultrasonic. Before deposition, the chamber was evacuated to a start pressure of 1.3×10^{-3} Pa and the substrate was heated to a temperature of 300 ℃. The deposition rates were 0.2 nm/s for HfO_2 and 0.5 nm/s for Al_2O_3, which were controlled by quartz crystal monitor system. After deposition, a tube furnace was used to conduct heat-treatment. The as-deposited thin films on MgF_2 substrates were simultaneously annealed at 600 ℃ for 1 h in air. These samples were classified into four series which noted as A1 for the as-deposited Al_2O_3 thin film, A2 for the Al_2O_3 thin film annealed at 600℃, AH1 for the as-deposited Al_2O_3 thin film with HfO_2 interlayer and AH2 for the Al_2O_3 thin film with HfO_2 interlayer annealed at 600℃.

Crystal structures of the thin films were characterized by grazing incidence X-ray diffractometry (GIXRD) using Cu Kα with an incident angle of 2°. The cross-sectional microstructure of the thin films were observed by a field emission scanning electron microscope (FE-SEM). The IR transmittance of the samples were measured by Fourier Transform Infrared (FTIR) spectrometer.

A commercial Nano Indenter system with a Berkovich indenter was employed to probe the hardness and modulus in the continuous stiffness measurement (CSM) mode. The maximum penetration depth was 1300 nm. Scratch tests were conducted by scratch components in the nanoindentation system. In the tests, a cubic-corner indenter was controlled to move at a constant velocity of 30 μm/s, while the normal load increased linearly with time. The maximum length and load were set at 500 μm and 500 mN, respectively. The critical loads (L_c) at which spallation occurred were also recorded.

2 Results and discussion

2.1 GIXRD, Microstructure and IR transmittance analysis

GIXRD patterns of the as-deposited and annealed films on MgF_2 substrates are represented in Fig. 1. For comparison, the main diffraction peaks of MgF_2 substrate and monoclinic HfO_2 are also exhibited at the bottom of the patterns. For samples A1, A2 and AH1, only the peaks of MgF_2 substrates can be observed, indicating amorphous structures of the thin films on the substrates. This illustrates that the annealing temperature (600℃) can't supply enough energy for the crystallization of Al_2O_3, for which the onset of crystallization was found to be around 800℃[18]. However, if the temperature was raised up to 700℃, the MgF_2 substrate was obviously damaged. While for sample AH2, there emerge some peaks around 24.6°, 28.3°, 31.7° and 50.9°, which correspond to (110), ($\bar{1}$11), (111) and ($\bar{1}$22) planes of HfO_2 monoclinic phase, respectively. It is noted that the temperature of phase transition from amorphous to monoclinic phase of HfO_2 thin film can be as low as 450℃[19].

Cross-sectional FE-SEM images of the as-deposited and annealed samples are shown in Fig. 2. A homogeneous structure with no obvious characteristics is observed in sample A1 (Fig. 2(a)), A2 (Fig. 2(b)), AH1 (Fig. 2(c)) and upper layer in AH2 (Fig. 2(d)), indicating that the thin films are all amorphous. Compared carefully, it is found that the amorphous structures in Fig. 2(b) and Fig 2(c) are more compact than that in Fig. 2(a). High temperature annealing makes the atoms move and thus the post annealed thin film becomes more compact. The more

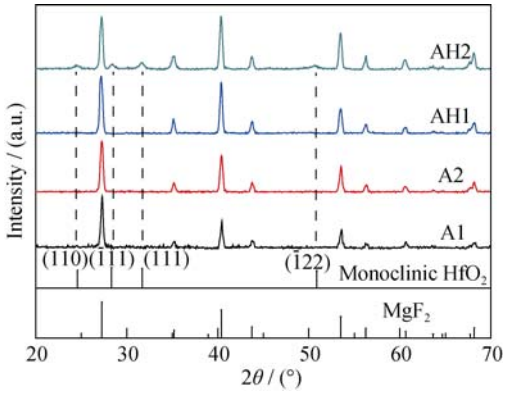

Fig. 1 GIXRD patterns of the as-deposited and annealed samples

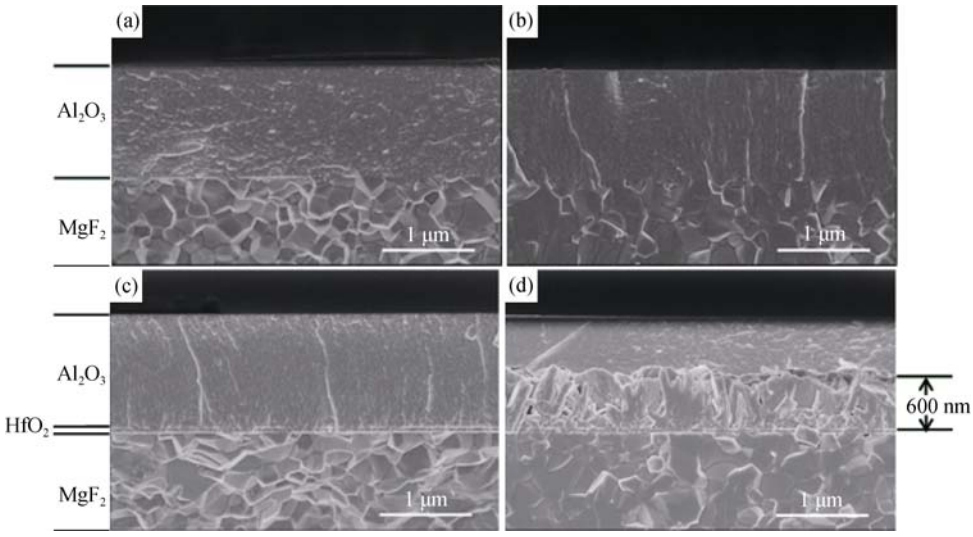

Fig. 2 Cross-sectional FE-SEM images of the as-deposited and annealed samples
(a) A1; (b) A2; (c) AH1; (d) AH2

compact structure of Al_2O_3 thin film grown on HfO_2 interlayer (AH1) might be caused by the surface effects of the pre-deposited HfO_2 thin film. But, for the annealed Al_2O_3 thin film with HfO_2 interlayer (AH2) in Fig. 2(d), there appears a new layer with branch-like structure between HfO_2 and upper Al_2O_3 thin film. In combination with GIXRD results above, there is no crystallization occurred for Al_2O_3 thin films. It is obvious that the phase transformation of HfO_2 interlayer from amorphous to monoclinic contributes to the formation of this new layer.

The transmittance spectra of the thin films as well as the MgF_2 substrate in the range of 3–5 μm are presented in Fig. 3. The average transmittance of 2 mm thick MgF_2 is about 95%. When deposited with Al_2O_3 thin film with a thickness of 1260 nm, the transmittance is reduced by 7%–17%. This transmittance loss is caused by the mismatch of the refractive indices, for the refractive index of MgF_2 is smaller than that of Al_2O_3. The transmittance in the whole range can be raised to varying degrees by annealing or introducing HfO_2 interlayer. This is due to the more compact microstructure or higher refractive index of HfO_2. However, the transmittance of AH2 is dramatically reduced by 15%–17%. It can be inferred that the strong absorption of the newly-formed layer with branch-like structure and the rough boundary generated in the middle of the film result in the reduction.

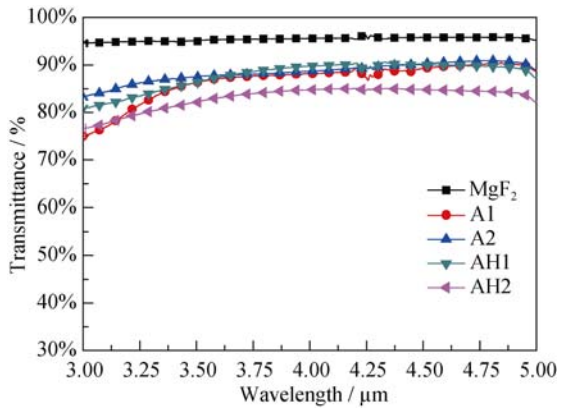

Fig. 3 IR transmittance spectra of the uncoated MgF_2, as-deposited and annealed samples in the range of 3–5 μm

2.2 Nanoindentation measurement

The elastic modulus and hardness of the thin films which are obtained as a function of penetration depth by CSM experiments are shown in Fig. 4(a) and Fig. 4(b), respectively. Elastic modulus curves in Fig. 4(a) tend to level off after reaching the maximum values except AH2, which has a larger peak and a following sharper decrease. The peak value equals to 205 GPa as compared with other three curves of 180 GPa. For hardness in Fig. 4(b), three regimes including initial rise, plateau and downturn can be recognized for the curves, which are typical characteristics of hard film on soft substrate[20]. Because of the round indenter tip, the initial contact with the surface is elastic, then the elastic zone increases with the penetration depth until a fully plastic zone is developed[21]. At this point, the hardness should reach a plateau. The downturn trends are ascribed to the influence of softer substrate which can be felt by the indenter at larger depth. The peak values of 12 GPa and 13.5 GPa are considered as the true hardness of as-deposited and annealed Al_2O_3 thin films, respectively. With the same annealing temperature and time, A2 exhibits a lower peak value of 13.5 GPa and a relatively flat slope. While AH2 undergoes a sharp increase to a peak value of 17.5 GPa at 30 nm and then falls off quickly to 12.5 Gpa at 300 nm. The peak values of 205 GPa and 17.5 GPa for AH2 are not the true elastic modulus and hardness of the upper layer or the newly formed layer. Because the upper layer with the featureless

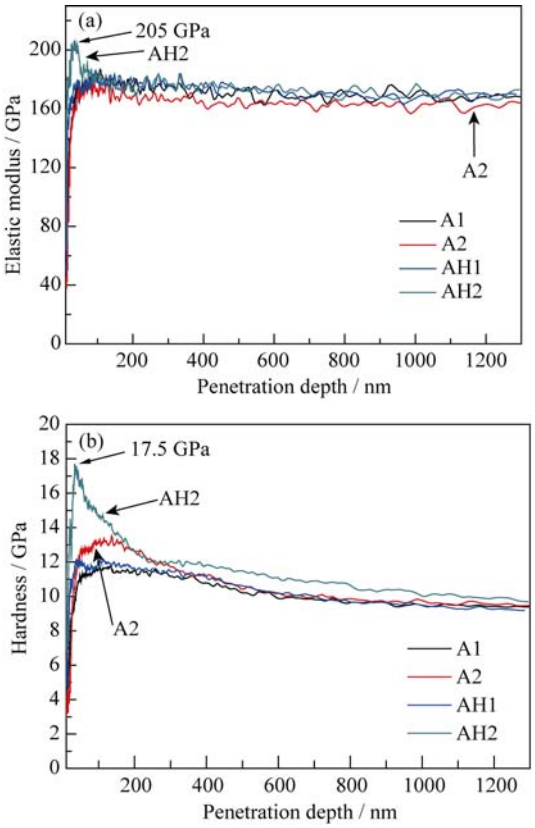

Fig. 4 Mechanical properties obtained from nanoindentation tests

(a) Elastic modulus as a function of penetration depth for as-deposited and annealed samples; (b) Hardness as a function of penetration depth for the same samples

and homogeneous microstructure is believed to be amorphous Al_2O_3, the abnormal increases of elastic modulus and hardness should be attributed to the newly formed layer below. As the indenter penetrates into the soft upper layer first, the peak values of 205 GPa and 17.5 GPa are considered to be decreased by the upper amorphous Al_2O_3 layer. So it can also be concluded that the true elastic modulus and hardness of the newly formed layer are lager than 205 GPa and 17.5 GPa, respectively.

2.3 Scratch tests

SEM surface micrographs of the scratch tracks on the as-deposited and annealed samples are shown in Fig. 5. For each track, it is intuitively seen that the width of groove trace increases with the increasing load until a large damage area appears at a certain point. The critical loads recorded at this point for A1, A2, AH1 and AH2 are 105 mN, 308 mN, 253 mN and 107 mN, respectively. The lower critical value of A1 could be attributed to high residual stress which can then be released by annealing or by introducing a HfO_2 interlayer. So the larger critical loads and smaller delaminated areas of A2 and AH1 are due to the stress relief. But the lower adhesion performance of AH2 is mainly because of the newly formed layer which may generate cracks in the middle of the film due to volume contraction. What A1 and AH2 have in common is that they possess almost the same critical load and same widespread delaminated area. For A1, spalling occurs in the form of ring-like cracks which are initiated by the tensile stress generated from friction at the tailing edge[22]. The extent of cracking is found to be not related with the applied load. When it begins to crack, the spalling area no longer expands with the increasing load for A1, A2 and AH1. While the spalling area even contracts with larger loads for AH2. When the applied load exceeds a certain value, the indenter gradually begins to penetrate into the substrate. Since the newly formed layer is much harder than the as-deposited or annealed Al_2O_3 thin films and could bear larger load, there is only groove generated on the substrate in Fig. 5(d), while the other three suffer more severe damages that some MgF_2 particles are drawn out. From the track edge in Fig. 5(d), there can be seen two different layers. In the higher resolution image of Fig. 5(e), the bare newly formed layer which is stripped off the upper layer is composed of randomly overlapped rods from a top view.

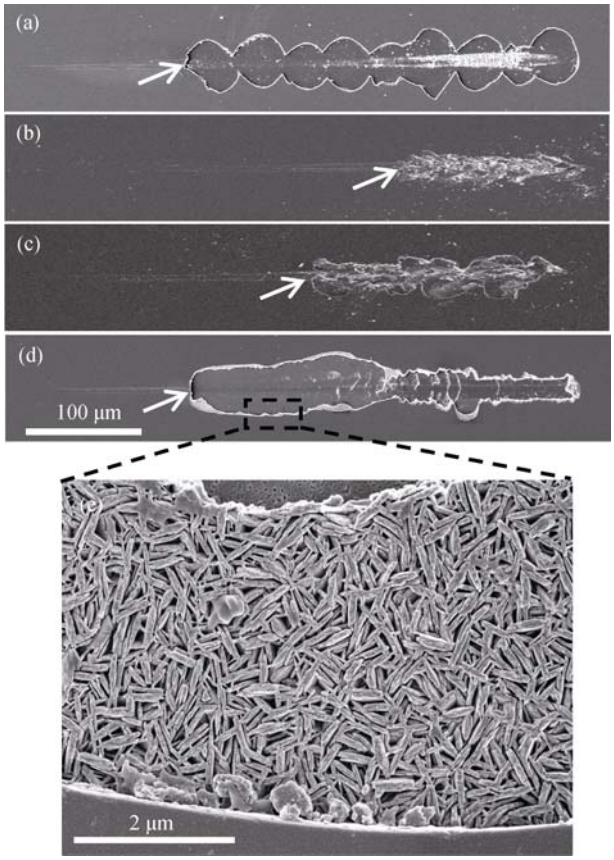

Fig. 5 SEM images of scratch tracks of the as-deposited and annealed samples.

(a) A1; (b) A2; (c)AH1; (d) AH2; (e) Higher resolution image of the selected area in Fig. 5(d)

3 Conclusions

Effects of HfO_2 interlayer on the crystalline phase, microstructure, IR transmittance and mechanical properties of Al_2O_3 thin film were studied. After annealing treatment, the Al_2O_3 thin film without HfO_2 interlayer remains amorphous, the elastic modulus stays the same while the hardness is increased from 12 GPa to 13.5 GPa. However, for the annealed Al_2O_3 thin film with a 50 nm HfO_2 interlayer between the substrate and Al_2O_3, a new layer with branch-like structure emerges in Al_2O_3. Two sharp peaks appear in the hardness and modulus curves. It can be inferred that the elastic modulus and hardness of the newly formed layer are larger than 205 GPa and 17.5 GPa, respectively. Additionally, it is also found that the new harder layer can help to protect the MgF_2 particles from being drawn out in scratch test. However, except the monoclinic peaks of HfO_2, there are no crystalline peaks found for Al_2O_3. This confirms that it is the HfO_2 phase transformation from amorphous to monoclinic that promotes the formation of the new layer.

References:

[1] MOGHIM M, PAYDAR M. Hot-pressing of bimodally distributed magnesium fluoride powder. *Infrared Physics & Technology*, 2010, **53(6):** 430–433.

[2] NOFAR M, HOSSEINI H M, SHIVAEE H. The dependency of optical properties on density for hot pressed MgF_2. *Infrared Physics & Technology*, 2008, **51(6):** 546–549.

[3] HI Q, LV F, ZHANG F, *et al*. Particle erosion of infrared materials. *Journal of University of Science and Technology Beijing, Mineral, Metallurgy, Material*, 2008, **15(6):** 758–763.

[4] ROBERTSON J. Diamond-like amorphous carbon. *Materials Science and Engineering: R: Reports*, 2002, **37(4):** 129–281.

[5] KISCHKAT J, PETERS S, GRUSKA B, *et al*. Mid-infrared optical properties of thin films of aluminum oxide, titanium dioxide, silicon dioxide, aluminum nitride, and silicon nitride. *Applied Optics*, 2012, **51(28):** 6789–6798.

[6] LI Y P, WANG N, CHE X S, *et al*. Infrared transmissive and rain-erosion resistant performances of GeC/GaP double-layer thin films on ZnS substrates. *Applied Surface Science*, 2013, **264:** 538–544.

[7] FENG L, LIU Z, LI Q, *et al*. Investigation of SiO_2/Si_3N_4 films prepared on sapphire by Rf magnetron reactive sputtering. *Applied Surface Science*, 2006, **252(12):** 4064–4070.

[8] KOHARA T, TAMAGAKI H, IKARI Y, *et al*. Deposition of α-Al_2O_3 hard coatings by reactive magnetron sputtering. *Surface and Coatings Technology*, 2004, **185(2):** 166–171.

[9] RUPPI S. Deposition, microstructure and properties of texture-controlled CVD α-Al_2O_3 coatings. *International Journal of Refractory Metals and Hard Materials*, 2005, **23(4):** 306–316.

[10] ZYWITZKI O, GOEDICKE K, MORGNER H. Structure and properties of Al_2O_3 layers deposited by plasma activated electron beam evaporation. *Surface and Coatings Technology*, 2002, **151:** 14–20.

[11] SHAMALA K, MURTHY L, RAO K N. Studies on optical and dielectric properties of Al_2O_3 thin films prepared by electron beam evaporation and spray pyrolysis method. *Materials Science and Engineering: B*, 2004, **106(3):** 269–274.

[12] ZHANG L, JIANG H, LIU C, *et al*. Annealing of Al_2O_3 thin films prepared by atomic layer deposition. *Journal of Physics D: Applied Physics*, 2007, **40(12):** 3707.

[13] MUSIL J, BLAŽEK J, ZEMAN P, *et al*. Thermal stability of alumina thin films containing γ-Al_2O_3 phase prepared by reactive magnetron sputtering. *Applied Surface Science*, 2010, **257(3):** 1058–1062.

[14] EKLUND P, SRIDHARAN M, SINGH G, *et al*. Thermal stability and phase transformations of γ-/amorphous-Al_2O_3 thin films. *Plasma Processes and Polymers*, 2009, **6(S1):** S907–S1011.

[15] RUPPI S, LARSSON A, FLINK A. Nanoindentation hardness, texture and microstructure of α-Al_2O_3 and κ-Al_2O_3 coatings. *Thin Solid Films*, 2008, **516(18):** 5959–5966.

[16] JIN P, XU G, TAZAWA M, *et al*. Low temperature deposition of a-Al_2O_3 thin films by sputtering using a Cr_2O_3 template. *Journal of Vacuum Science & Technology A Vacuum, Surfaces, and Films*, 2002, **20(6):** 2134–2136.

[17] PANG X, GAO K, LUO F, *et al*. Annealing effects on microstructure and mechanical properties of chromium oxide coatings. *Thin Solid Films*, 2008, **516(15):** 4685–4689.

[18] LEE S K, LEE S B, PARK S Y, *et al*. Structure of amorphous aluminum oxide. *Physical Review Letters*, 2009, **103(9):** 095501.

[19] HE Q, GUO H B, WEI J J, *et al*. Deposition of HfO_2 thin films on ZnS substrates. *Thin Solid Films*, 2008, **516(15):** 4695–4699.

[20] FISCHER-CRIPPS A C. Critical review of analysis and interpretation of nanoindentation test data. *Surface and Coatings Technology*, 2006, **200(14):** 4153–4165.

[21] LI X, BHUSHAN B. A review of nanoindentation continuous stiffness measurement technique and its applications. *Materials Characterization*, 2002, **48(1):** 11–36.

[22] BORRERO-LOPEZ O, HOFFMAN M. Measurement of fracture strength in brittle thin films. *Surface and Coatings Technology*, 2014, **254:** 1–10.

氟化镁基底上 HfO_2 中间层对 Al_2O_3 薄膜微观组织和力学性能的影响

宋 博[1,2], 赵丽丽[1], 陈笑迎[1], 游丽君[1], 宋力昕[1]

(1. 中国科学院 上海硅酸盐研究所, 特种无机涂层重点实验室, 上海 200050; 2. 中国科学院大学, 北京 100049)

摘 要: 采用电子束蒸镀技术在氟化镁基底上制备了单层 Al_2O_3 薄膜和含有 HfO_2 中间层的 HfO_2/Al_2O_3 双层薄膜。在空气中对所制备的薄膜进行 1 h 600℃的退火处理。通过掠入角 X 射线衍射仪(GIXRD)、场发射扫描电镜(FE-SEM)、傅里叶变换红外光谱仪(FTIR)、纳米压痕和划痕法对薄膜的微观结构、红外透过率和力学性能进行了表征。结果表明: 退火处理后 HfO_2/Al_2O_3 双层薄膜中形成了一层树枝状的新层, 这种新层的硬度大于 17.5 GPa。这种高硬度的新层能够保护氟化镁基底不被划伤。从 GIXRD 图谱中只能找到单斜相 HfO_2 的衍射峰, 而 Al_2O_3 薄膜仍然保持非晶态。从这些结果中可以推断出 HfO_2 从非晶态向单斜相的转变促进了这种树枝状新层的产生, 也正是这种新层提高了保护薄膜的力学性能。

关 键 词: HfO_2 中间层; Al_2O_3 薄膜; 微观组织; 力学性能; 氟化镁基底

中图分类号: TQ174 **文献标识码:** A